

Table 2. Measured and calculated ratios  $I_{\text{TDS}}^B/I_{\text{TDS}}^{\text{tot}}$ 

$I_{\text{TDS}}^B$  is the integrated first-order TDS intensity included in the background,  $I_{\text{TDS}}^{\text{tot}}$  is the integrated first-order TDS intensity included in the Bragg peak. Scan length  $2 \cdot 0^\circ$ .

Reflection	Measured	Calculated <sup>a</sup> approximation		Numerical calculations		
		cylinder	sphere	St <sup>b</sup>	H & V <sup>c</sup>	K & M <sup>d</sup>
030	0.52 (7)	0.15	0.33	0.574	0.577	0.577
060	0.56 (9)	0.32	0.33	0.497	0.498	0.498

Calculated after: (a) Willis (1969); (b) Stevens (1974); (c) Helmholtz & Vos (1977); (d) Kurittu & Merisalo (1977).

TDS contribution can be taken into account by these first-order TDS calculations with an accuracy of approximately 4%.

Assuming that (i) the harmonic approximation is valid, (ii) the influence of the radiation damage on the diffuse intensities is negligible and (iii) the first-order TDS is still the most dominant contribution, a mean temperature factor  $B$  can be determined from the measured inelastic intensities of at least two reflections with parallel scattering vectors  $S$  (for details see Krec & Steiner, 1984). The measured inelastically scattered radiation included in the Bragg peak was integrated after subtracting the contribution in the background. The resulting integrated intensity was corrected for second-order TDS contributions, the amount of which was estimated with the program *TDS2* written by Stevens (1974). From the ratio of the resulting diffuse intensities of the two reflections  $B$  was determined using the known structure factors  $F_o$ . The obtained  $B$  values at 295 K are 0.37 (8) and 0.33 (8)  $\text{\AA}^2$  for the cylindrical and spherical approximations used for the calculation of the illuminated volume and are in agreement with the one reported by Fujimoto (1982) measured in the hexagonal  $Z$  direction.

#### References

ABRAHAMS, S. C., REDDY, J. M. & BERNSTEIN, J. L. (1966). *J. Phys. Chem. Solids*, **27**, 997–1012.

- CHOWDHURY, M. R., PECKHAM, G. E. & SAUNDERSON, D. H. (1978). *J. Phys. C*, **11**, 1671–1683.
- DATE, S. K., GONSER, U. & KEUNE, W. (1979). *Hyperfine Interact.* **7**, 369–375.
- DATE, S. K., JOAG, P. S., ENGELMANN, H., KEUNE, W. & GONSER, U. (1981). *Ferroelectrics*, **31**, 5–10.
- FUJIMOTO, I. (1982). *Acta Cryst.* **A38**, 337–345.
- HELMHOLDT, R. B. & VOS, A. (1977). *Acta Cryst.* **A33**, 38–45.
- International Tables for X-ray Crystallography* (1974). Vol. IV, edited by J. A. IBERS & W. HAMILTON, pp. 99–101. Birmingham: Kynoch Press.
- KREC, K. & STEINER, W. (1984). *Acta Cryst.* **A40**, 459–465.
- KURITTU, J. & MERISALO, M. (1977). *Report Series in Physics*, No. 132, Univ. of Helsinki.
- LAUER, J., PFANNES, H. D. & KEUNE, W. (1979). *J. Phys. (Paris)*, **40**, C2–561–563.
- LEHMANN, M. S. (1980). *Electron and Magnetisation Densities in Molecules and Crystals*, edited by P. BECKER, pp. 287–322. New York: Plenum Press.
- PFANNES, H. D., LAUER, J., KEUNE, W., MAEDA, Y. & SAKAI, H. (1980). *J. Phys. (Paris)*, **41**, C1–453–454.
- PONGRATZ, P., CERVA, H., SKALICKY, P., OPPOLZER, H. & WILLIBALD, E. (1982). *Proc. 10th Int. Congr. on Electron Microscopy*.
- RAUBER, A. (1978). *Chemistry and Physics of LiNbO<sub>3</sub>. Current Topics in Material Science*, Vol. 1. Amsterdam: North Holland.
- SARAVIA, L. R. & ELLIS, S. C. (1966). *Acta Cryst.* **20**, 927–930.
- SCHNEIDER, J. R. (1980). *Characterisation of Crystal Growth Defects by X-ray Methods*, edited by B. K. TANNER & D. K. BOWEN, pp. 186–215. New York: Plenum Press.
- SMITH, R. T. & WELSH, F. S. (1971). *J. Appl. Phys.* **42**, 2219–2230.
- STEVENS, E. D. (1974). *Acta Cryst.* **A30**, 184–189.
- WILLIBALD, E. (1981). Private communication.
- WILLIS, B. T. M. (1969). *Acta Cryst.* **A25**, 277–300.

*Acta Cryst.* (1984). **A40**, 468–473

## Signal, Noise and Resolving Power in Rotation Searches

BY G. H. PETIT,\* H. J. GEISE AND A. T. H. LENSTRA†

*University of Antwerp (UIA), Department of Chemistry, Universiteitsplein 1, B-2610 Wilrijk, Belgium*

(Received 6 October 1983; accepted 20 March 1984)

### Abstract

First and second moments of the probability density of the function  $R = \sum_H E_o^2 E_c^2$  are evaluated for  $n$ -atom

models consisting of  $i$  correctly and  $n - i$  incorrectly placed atoms of an  $N$ -atom structure. Formulas are valid for space groups  $P1$  and  $P\bar{1}$ , and describe the influence of the size of the model as well as data truncation. Introduction of the concept of an averaged structure leads to structure-independent conclusions about the behaviour of the resolving

\* Present address: Bell Telephone Manufacturing Company, Francis Wellesplein, Antwerpen, Belgium.

† Author to whom correspondence should be addressed.

power of the product function  $R$  in rotation searches. The signal (model with  $i = n$ ) stands out more clearly against the random noise (models with  $i = 0$ ) when intensities below a certain threshold are removed from the data set. Results are verified against simulated experiments as well as a real structure.

### Introduction

The proper orientation of a known molecular fragment may be determined using as discriminator the function

$$R = \sum_H E_o^2(H)E_c^2(H). \quad (1)$$

$E_o$  and  $E_c$  are the normalized structure factors belonging to the structure and the search fragment, respectively. The rotation search is successful if the largest observed  $R$  value corresponds to the correct orientation and is not one of the  $R$  values belonging to the multitude of completely and partly incorrect orientations. Therefore, the question under what conditions (1) is a useful discriminator function can only be answered from knowledge of the probability density function  $P(R)$ . An example in the form of a histogram is given in Fig. 1.

In this paper we investigate by theoretical statistical methods the properties of  $P(R)$  via its moments. In particular, the effect of the size of the search fragment and the effects of data truncation will be described. We will assume that the data are error free and will restrict ourselves to the space groups  $P1$  and  $P\bar{1}$  and to search models for which all intramolecular vectors are correct in magnitude. Thus we exclude models containing some position which is not superimposable upon the unknown structure.

It will be convenient to have at our disposal a short and concise nomenclature for common crystallographic situations. An  $n$ -atom search model contain-

ing  $i$  correctly and  $n - i$  incorrectly oriented atoms will be denoted by  $(i, n - i)$  with  $n \leq N$ , the number of atoms in the structure. The total assembly of  $R$  values is then considered as the set of the probability densities of  $R$  values belonging to various crystallographic situations, i.e.  $P(R) = P[R(i, n - i)]$ .

We distinguish three cases:

(i) the correct orientation  $(n, 0)$ , the corresponding  $R(n, 0)$  is called the signal and will be single valued for a particular structure with a particular search fragment.

(ii) all completely incorrect orientations  $(0, n)$ , the contribution of which to  $P(R)$  is called the random noise.

(iii) partly correct orientations  $(i, n - i)$ , the contributions of which are called the non-random noise.

The density functions are then defined over the sample space of all possible search-fragment orientations  $(i, n - i)$  of a particular structure.

If an orientation  $(i, n - i)$  can be realized in a large number of ways, the corresponding  $P[R(i, n - i)]$  can be considered as a continuous function. In a particular structure with a given search fragment this is true for the random noise, because orientations  $(0, n)$  can be realized in a quasi-infinite number of ways. For other orientations – the non-random noise – this is not so and the corresponding  $P[R(i, n - i)]$  becomes discrete and depends very much upon the actual choice of the search fragment.

Since we want to arrive at general structure-independent conclusions, we will in our approach perform an extra averaging over all possible observable structures. We will show that the average structure thus defined describes the situation for a particular structure rather well for the signal and the random noise. The (Gaussian) shape of the latter can be predicted accurately. The structure- and search-fragment-dependent peculiarities of an actual structure, however, prevent an adequate statistical analysis of the non-random noise via the concept of the average structure.

### Algebraic derivations

Until recently, it was not possible to predict meaningful spreads (second moments) of the probability function  $P[R(g, f)]$ . Van Havere & Lenstra (1983a, b, c) showed that the problems could be overcome by using the concept of conditional probabilities. For the fundamentals as well as for evidence of the validity of the assumptions used in the new theory, we refer to Van Havere & Lenstra. With general validity the first and second moments of  $P(R)$  can be written as

$$\langle R; E_o^2 \rangle = \sum_H E_o^2 \langle E_c^2; E_o^2 \rangle \quad (2)$$

and

$$\sigma^2(R; E_o^2) = \sum_H E_o^4 [\langle E_c^4; E_o^2 \rangle - \langle E_c^2; E_o^2 \rangle^2]. \quad (3)$$

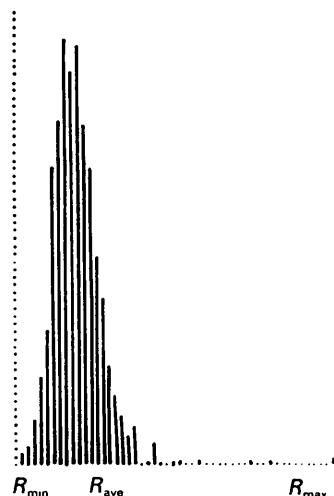


Fig. 1. Density distribution of  $R$  values normally encountered in a rotation search.

Table 1. *The evaluation of*  $\langle E_o^p \rangle_a$ 

	Space group $P1$	Space group $P\bar{1}$
$\langle E_o^2 \rangle_a$	$1+a$	$1+Q$
$\langle E_o^4 \rangle_a$	$2+2a+a^2$	$3+(3+a)Q$
$\langle E_o^6 \rangle_a$	$6+6a+3a^2+a^3$	$15+(15+5a+a^2)Q$
$\mathcal{H}_a$	$\mathcal{H}e^{-a}$	$\mathcal{H}\text{erfc}(a/2)^{0.5}$
	$Q = (2a/\pi)^{0.5} e^{-(a/2)/\text{erfc}(a/2)^{0.5}}$	

The notation  $\langle A; E_o^2 \rangle$  means the value  $A$  averaged over all orientations of the search fragment under the constraint of  $E_o^2$ , the set of observed  $E^2$  values. The conditional notation of the intensity moments, e.g.  $\langle E_c^4; E_o^2 \rangle$ , shows that the available data are taken as a set of fixed parameters, representing the structure at hand.

Expressions for  $\langle E_o^2; E_c^2 \rangle$  and  $\langle E_o^4; E_c^2 \rangle$  for the general situation ( $g, f$ ) in the space groups  $P1$  and  $P\bar{1}$  can easily be derived following the procedure of Petit & Lenstra (1982). Since the roles of  $E_o^2$  and  $E_c^2$  can be interchanged (Srinivasan & Parthasarathy, 1976), it follows that the moments  $\langle E_c^2; E_o^2 \rangle$  and  $\langle E_c^4; E_o^2 \rangle$  can be readily obtained. One thus finds

$$\langle E_c^2; E_o^2 \rangle = \frac{g^2}{nN} E_o^2 + 1 - \frac{g^2}{nN} \quad (4)$$

$$\langle E_c^4; E_o^2 \rangle = (g^4/n^2N^2)E_o^4 + 2\alpha(1-g^2/nN)(g^2/nN)E_o^2 + \alpha(1-g^2/nN)^2 \quad (5)$$

(it is assumed that  $g, n$  and  $N$  are large). Analogous formulas were derived by Van Havere & Lenstra (1983c). Equation (4) is valid for  $P1$  as well as for  $P\bar{1}$ , while (5) holds for  $P1$  if  $\alpha = 2$  and for  $P\bar{1}$  if  $\alpha = 3$ .

Substitution of (4) and (5) in (2) and (3) yields

$$\langle R; E_o^2 \rangle = \frac{1}{nN} \sum_H \{g^2 E_o^4 + (nN - g^2) E_o^2\} \quad (6)$$

$$\sigma^2(R; E_o^2) = \frac{1}{n^2 N^2} \sum_H \{2(\alpha - 1)g^2(nN - g^2)E_o^6 + (\alpha - 1)(nN - g^2)^2 E_o^4\}. \quad (7)$$

Now we can introduce the effects of data truncation by defining a threshold  $a$ , below which intensities are omitted from the calculations. In mathematical terms, it means

$$\sum_H E_o^p; a \leq E_o^2 \quad \text{or} \quad \mathcal{H}_a \langle E_o^p \rangle_a$$

The averaging brackets indicate the averaging over all reflections above  $a$  and the subscript  $a$  is here linked to that threshold value.  $\mathcal{H}$  and  $\mathcal{H}_a$  are, respectively, the number of reflections before and after the threshold is applied.

Equations (6) and (7) are still valid in the particular case of a single structure under investigation. We now generalize the picture, i.e. without reference to an actual structure, by replacing  $\sum_H E_o^p; a \leq E_o^2$  or

$\mathcal{H}_a \langle E_o^p \rangle_a$  by their distribution values. In this way an extra averaging over all possible observable structures is introduced. So  $\mathcal{H}_a$  and  $\langle E_o^p \rangle_a$  can be found by evaluating

$$\mathcal{H}_a = \mathcal{H} \int_{a^{1/2}}^{\infty} P(E_o) dE_o \quad (8)$$

and

$$\langle E_o^p \rangle_a = \int_{a^{1/2}}^{\infty} E_o^p P(E_o) dE_o / \int_{a^{1/2}}^{\infty} P(E_o) dE_o. \quad (9)$$

The marginal probability density functions  $P(E_o)$  for the space groups  $P1$  and  $P\bar{1}$  are given by Wilson (1949) for structures containing a large number of atoms.

It has been shown (Van Havere & Lenstra, 1983a) that the asymptotic Wilson distribution is sufficiently accurate in most practical situations. Technical details on the evaluation of the integrals (9) are reported by Petit, Lenstra & Van Loock (1981). The results are summarized in Table 1. It should be noted that the production of the Wilson intensity statistics, i.e.  $\langle E^2 \rangle = 1$ , renders the results of this investigation only valid for data sets that allow an atomic resolution.

Finally, by substitution of the appropriate moments into (6) and (7) we arrive at the first and second moments of  $P[R(g, f)]$  for an averaged structure taking into account the effect of data truncation and using a search fragment in the situation ( $g, f$ ). So for  $P1$  we have

$$\langle R; E_o^2 \rangle = \frac{\mathcal{H}e^{-a}}{nN} \{g^2(1+a+a^2) + (1+a)nN\} \quad (10)$$

$$\sigma^2(R; E_o^2) = \mathcal{H}e^{-a} [(nN - g^2)/n^2 N^2] \times \{g^2(10+10a+5a^2 + 2a^3) + nN(2+2a+a^2)\}. \quad (11)$$

Similarly, we obtain the moments for an averaged structure in  $P\bar{1}$ :

$$\langle R; E_o^2 \rangle = \{\mathcal{H}\text{erfc}(a/2)^{0.5}/nN\} \{g^2(2+2Q+aQ) + nN(1+Q)\} \quad (12)$$

$$\sigma^2(R; E_o^2) = 2\mathcal{H}\text{erfc}(a/2)^{0.5} [(nN - g^2)/n^2 N^2] \times \{g^2(27+27Q+9aQ+2a^2Q) + nN(3+3Q+aQ)\}. \quad (13)$$

Obviously, the formulas for the correct orientation can be obtained from (10) to (13) by putting  $g = n$ , while those for the random noise are obtained by putting  $g = 0$ . It follows that  $R(n, 0)$  is always larger than  $R(0, n)$ , with in between values for  $R(g, f)$ .

### The resolving power of the product function

The above results may serve to estimate the resolving power  $D_a$  of the rotation function (1) to discriminate

the signal from the random noise. We define

$$D_a = \frac{\langle R(n, 0) \rangle_a - \langle R(0, n) \rangle_a}{\varepsilon \sigma_a(0, n)} \quad (14)$$

$\sigma_a$  is a value related to the number of reflections and  $\varepsilon$  depends on the number of rotation search points taken. For a standard structure  $\varepsilon$  can be taken between 2 and 3.

A contribution containing  $\sigma_a(n, 0)$  is omitted from the denominator of (14) because in each particular rotation search there is only one perfectly fitting orientation of the search fragment, *i.e.*  $\sigma_a(n, 0)$  may be taken as zero.

Substitution of the relevant equations yields

$$D_a = \mathcal{H}^{0.5} (n/\varepsilon N) Z_a \quad (15)$$

with

$$Z_a = \frac{(1+a+a^2)(e^{-a})^{0.5}}{(2+2a+a^2)^{0.5}} \quad \text{in } P1 \quad (16)$$

and

$$Z_a = \frac{[2+(2+a)Q][\text{erfc}(a/2)^{0.5}]^{0.5}}{2^{0.5}\{3+(3+a)Q\}^{0.5}} \quad \text{in } P\bar{1}. \quad (17)$$

It follows that the resolving power is proportional to the size of the search fragment relative to the size of the structure ( $n/N$ ) and is proportional to the square root of the number of observable reflections ( $\mathcal{H}$ ). These facts are well known to the crystallographer.

Somewhat more surprising is the behaviour of  $Z_a$ , and thus of  $D_a$ . The path of  $Z_a$  as a function of the threshold is depicted in Fig. 2, showing a maximum at  $a = 1.485$  for  $P1$  and at  $a = 1.608$  for  $P\bar{1}$ .

Obviously, the usefulness of  $D_a$  lies in the fact that  $D_a$  values greater than 1 indicate that the orientation search will proceed in a straightforward manner: the maximum  $R$  value corresponding to the proper orientation is well separated from the random noise.

On the other hand, if  $D_a < 1$  a quasi certain failure of the rotation search is expected. In view of this some important conclusions can be made.

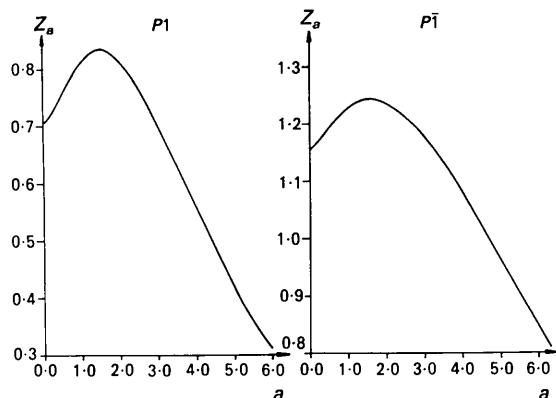


Fig. 2. Behaviour of  $Z_a$  as a function of the threshold  $a$  for an averaged structure in  $P1$  (left) and  $P\bar{1}$  (right).

(i) The elimination of low intensities up to  $a = 2.975$  and  $a = 3.275$  for  $P1$  and  $P\bar{1}$ , respectively, does not lower the resolving power below the level of  $D$  at  $a = 0$ . This phenomenon explains the common empirical observation that the exact orientation parameters can still be found if one uses only the strongest 10% reflections (*e.g.* Tollin & Rossmann, 1966; Hill, Tsernoglou & Banaszak, 1973). Of course, in cases where  $D > 1$ , the availability of fast computers and fast Fourier techniques make it no longer desirable to speed up the calculations by eliminating part of the intensities.

(ii) If, however, only a search fragment is available leading to  $D_{a=0} < 1$ , the discriminating power of the rotation search can be increased by eliminating all intensities below  $a = 1.485$  for  $P1$  and  $a = 1.608$  for  $P\bar{1}$ , thereby increasing  $D_a$  by approximately 20 and 10%, respectively. Equivalent to elimination is to put all intensities below the above mentioned thresholds equal to zero.

(iii) The behaviour of  $Z_a$  (and of  $D_a$ ) is largely determined by the behaviour of the numerators in (17) and (16), since they contain the higher power in  $a$  compared to the denominator. Inspection of the numerator  $T$  with reference to (6) shows that  $T$  can be written as

$$T = \frac{n}{N} \sum_H E_o^2 (E_o^2 - 1). \quad (18)$$

Equation (18) expresses mathematically that all  $E_o^2 < 1$  give a negative contribution to the sum, whereas all  $E_o^2 > 1$  give a positive contribution. Hence, elimination of intensities  $E_o^2 < 1$  will increase  $T$ . This corresponds to the removal of the origin peak in the observed Patterson map. An origin-removed Patterson often reveals structural details more easily than the original. Owing to the presence of  $\sigma(R)$  in the denominator of (14), the maximum of  $D_a$  is slightly shifted to higher  $a$  values.

(iv) The concept of the average structure was introduced to allow general structure-independent conclusions. For an actual structure  $D_a$  can be estimated *a priori* with higher accuracy by using in (6) and (7) the actual values of  $\sum_H E_o^6$ ,  $\sum_H E_o^4$  and  $\sum_H E_o^2$  of the structure at hand. In that way, structure-dependent features can be introduced in *all* our expressions.

### Experimental verification

Flaws in the way of reasoning and in the derivation of a statistical theory can best be investigated by comparing the theoretical results with those obtained after averaging over a sufficiently large number of simulated experiments. When agreement exists one may still ask whether the theory, however correct for the average structure, will be useful in the case of a particular structure. Then one questions the robustness of the predictions towards the peculiarities of a

Table 2. Comparison between experimental (simulated) and theoretical values for  $\mathcal{H}_a$ ,  $R(n, 0)$ ,  $R(0, n)$ ,  $\sigma^2(0, n)$  and  $D_a$  at various values of the threshold  $a$  for an averaged structure in P1

$a$	$\mathcal{H}_a$		$R(n, 0)$		$R(0, n)$		$\sigma(0, n)$		$D_a$	
	exp.	theor.	exp.	equation (10)*	exp.	equation (10)†	exp.	equation (11)‡	exp.	equation (14)
0	960.0	960.0	1657.9	1680.0	968.6	960.0	41.3	43.8	5.53	5.48
1	356.8	353.2	1481.1	1501.1	714.7	706.4	41.8	42.0	6.15	6.30
2	130.9	129.9	1044.7	1071.7	392.4	389.7	36.5	36.0	5.94	6.31
3	47.2	47.8	624.4	657.3	188.9	191.2	28.7	28.5	5.06	5.45
4	16.2	17.6	325.3	365.2	81.0	88.0	20.8	21.4	3.92	4.32
5	5.7	6.5	160.8	190.1	34.3	39.0	15.6	15.5	2.70	3.24

\* With  $g = n = 30$  and  $N = 40$ .  
 † With  $g = 0, n = 30$  and  $N = 40$ .  
 ‡ With  $g = 0, n = 30$  and  $N = 40$ .

real structure, peculiarities which are not explicitly modelled into the theory. For example, we ignored in our derivations the effects of measuring errors and the effects of small misplacements in the atomic coordinates. We will therefore examine in detail our theoretical results in the case of P1 against a simulated averaged structure as well as against an actual molecule.

**Verification against simulated structures**

Simulations were performed over a series of 100 structures in P1. Each single structure contained 40 equal atoms with a corresponding data set of 960 reflections. The search fragment contained 30 atoms in all cases. We tested only the behaviour as a function of data truncation, since the behaviour as a function of the model size has already been examined (Van Havere & Lenstra, 1983a, b, c) for the closely related  $R_2$  values. For computation economics all calculations were performed in two dimensions, so that there was only one rotation parameter. Structures and search fragments were generated randomly and each search fragment was rotated in its asymmetric part. It was decided to stop the simulations after 100 structures since comparison of the results with those obtained after 50 structures revealed no serious differences. Nevertheless, the length of the series (100 structures) as well as the size of the structures (40 atoms) are rather small, but are dictated by the limits set by the computer facilities.

The maximum value of  $R(R_{max})$  and the value of  $R$  averaged over all rotation grid points ( $R_{ave}$ ) were taken. Then  $\langle R_{max} \rangle$ ,  $\langle R_{ave} \rangle$  and  $s^2(R)$  were calculated from

$$\langle R_{max} \rangle = \sum_{100} R_{max}/100, \quad \langle R_{ave} \rangle = \sum_{100} R_{ave}/100$$

$$s^2(R) = \sum_{100} \{ \langle R^2 \rangle - \langle R_{ave} \rangle^2 \} / 100.$$

$\langle R_{max} \rangle$  is to be compared with  $R(n, 0)$ ,  $\langle R_{ave} \rangle$  with  $R(0, n)$ , both calculated from (10), while  $s^2(R)$  is to be compared with  $\sigma^2(0, n)$ , calculated from (11). Table 2 gives the comparison of these quantities

together with  $\mathcal{H}_a$  and  $D_a$  as a function of the threshold  $a$ .

The occurrence of a maximum in  $D_{exp}$  near  $a = 1.5$  is clearly visible. The overall agreement is satisfactory, taking into account the smallness of the numbers in the simulation set. Their influence is discussed by Van Havere & Lenstra (1983a).

**Verification against a real structure**

The theoretical expressions were tested against a real structure, taking ammonium hydrogen malate in P1 (Versichel, Van de Mieroop & Lenstra, 1978) as test example. Fig. 3 shows the experimental histogram of  $R$  values – obtained after a Lattmann (1972) rotation search – upon which are superposed the theoretical signal and the theoretical Gaussian describing the random noise of the average structure [(10) and (11)].

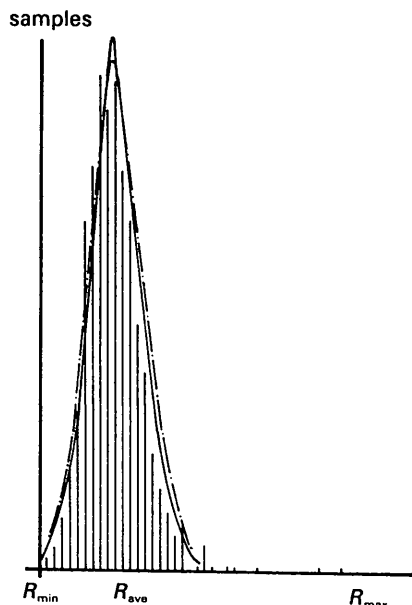


Fig. 3. Comparison between the theoretical Gaussian distribution describing the random noise for the average structure (—), the random noise predicted using the actual data set (---) and the corresponding experimental histogram for ammonium hydrogen malate.

No attempt was made to include contributions of non-random noise in the theoretical curve.

The agreement is satisfactory and indicates the robustness of the average structure concept. In fact, other examples, not given here, show that the agreement of first moments is as striking as was observed previously for the  $R_2$  function (Petit, Lenstra & Van Loock, 1981).

Fig. 3 also shows that an even better prediction of the signal and the random noise can be made by using in (6) and (7) the actual sums  $\sum_H E_o^p$  of the experimental data set.

#### References

HILL, E. J., TSEBNOGLOU, D. & BANASZAK, L. J. (1973). *Acta Cryst.* **B29**, 921–922.

LATTMANN, E. E. (1972). *Acta Cryst.* **B28**, 1065–1068.

PETIT, G. H. & LENSTRA, A. T. H. (1982). *Acta Cryst.* **A38**, 67–70.

PETIT, G. H., LENSTRA, A. T. H. & VAN LOOCK, J. F. (1981). *Acta Cryst.* **A37**, 353–360.

SRINIVASAN, R. & PARTHASARATHY, S. (1976). In *Some Statistical Applications in X-ray Crystallography*, p. 84. Oxford: Pergamon.

TOLLIN, P. & ROSSMANN, M. G. (1966). *Acta Cryst.* **21**, 872–876.

VAN HAVERE, W. K. L. & LENSTRA, A. T. H. (1983a). *Acta Cryst.* **A39**, 553–562.

VAN HAVERE, W. K. L. & LENSTRA, A. T. H. (1983b). *Acta Cryst.* **A39**, 562–565.

VAN HAVERE, W. K. L. & LENSTRA, A. T. H. (1983c). *Acta Cryst.* **A39**, 847–853.

VERSICHEL, W., VAN DE MIEROOP, W. & LENSTRA, A. T. H. (1978). *Acta Cryst.* **B34**, 2643–2645.

WILSON, A. J. C. (1949). *Acta Cryst.* **2**, 318–321.

*Acta Cryst.* (1984). **A40**, 473–482

## An Aid to the Structural Analysis of Incommensurate Phases

By J. D. C. McCONNELL

*Department of Earth Sciences, Downing Street, Cambridge CB2 3EQ, England and Schlumberger Cambridge Research, PO Box 153, Cambridge CB2 3BE, England*

AND VOLKER HEINE

*Cavendish Laboratory, Madingley Road, Cambridge CB2 0HE, England*

(Received 13 February 1984; accepted 6 March 1984)

#### Abstract

Group theory is used to establish three results likely to be useful in solving the crystal structures of complicated incommensurate phases. In the first of these it is demonstrated that an incommensurate structure with paired scattering vectors  $\pm\mathbf{q}$  must contain two different component structures, one modulated with  $\cos\mathbf{q}\cdot\mathbf{r}$  and the other with  $\sin\mathbf{q}\cdot\mathbf{r}$ . The second theorem states that the two components have different but related symmetries if the average structure has at least one element in its space group which turns  $\mathbf{q}$  into  $-\mathbf{q}$ . In that case, each aspect of the modulation is assigned uniquely by symmetry to either the cosine or sine factor. The third result concerns the Patterson function that may be constructed from the intensity scattered by the incommensurate modulation. This is also necessarily two-dimensional, the plus difference Patterson function being the sum of the Patterson functions obtained separately for the two component structures, while the minus difference Patterson function contains cross terms between the two components. Other symmetry arguments are mentioned, including symmetry signatures in Patterson functions, and systematic equalities in satellite intensities which

arise from systematic extinctions in the scattering from one component or the other.

#### 1. Introduction: the use of two-component structures

This paper is concerned with the ramifications of one basic point, that the structure of a modulated incommensurate (IC) phase can always be expressed in the form of two components:

$$\begin{aligned} (\text{IC structure}) = & (\text{average structure}) \\ & + (\text{first component } C_1) \times \cos \mathbf{q} \cdot \mathbf{r} \\ & + (\text{second component } C_2) \times \sin \mathbf{q} \cdot \mathbf{r}. \end{aligned} \quad (1.1)$$

This has a number of advantages which we shall develop, especially for solving complicated IC structures such as some minerals. We emphasize that on general group-theoretical grounds there can be, and so presumably usually are, *two* independent modulation component structures ('components' for short)  $C_1$  and  $C_2$  oscillating  $90^\circ$  out of phase with one another in (1.1) (McConnell, 1978, 1981a). Fig. 1 illustrates the situation. Much of the utility of this